Carbohydrate Polymers 117 (2015) 169–176

Contents lists available at ScienceDirect

Carbohydrate Polymers

journal homepage: www.elsevier.com/locate/carbpol

Characterization and antioxidant activity of β-carotene loaded chitosan-graft-poly(lactide) nanomicelles

Wenjiao Ge[a], Dong Li[a], Meiwan Chen[b], Xiaohui Wang[a,*], Shijie Liu[a], Runcang Sun[a,c]

[a] State Key Laboratory of Pulp and Paper Engineering, South China University of Technology, Guangzhou 510640, China
[b] State Key Laboratory of Quality Research in Chinese Medicine, Institute of Chinese Medical Sciences, University of Macau, Macau 999078, China
[c] Institute of Biomass Chemistry and Technology, Beijing Forestry University, Beijing 100083, China

ARTICLE INFO

Article history:
Received 17 May 2014
Received in revised form
15 September 2014
Accepted 17 September 2014
Available online 28 September 2014

Keywords:
Chitosan
Self-assemble
Nanomicelles
β-Carotene
Antioxidant activity

ABSTRACT

β-Carotene (β-C) is a well-established natural antioxidant agent, but its poor water-solubility, low chemical stability and low bioavailability limit its application in food, pharmaceuticals and cosmetics industries. Thus it is critical to develop an efficient method to improve the water solubility and stability of β-C. In this research, amphiphilic chitosan-graft-poly (lactide) (CS-g-PLA) copolymer was synthesized via a homogeneous ring-opening polymerization (ROP) in ionic liquid. The obtained CS-g-PLA copolymer was able to self-assemble into about 14 nm micelles in water at low concentration, and β-C loaded micelles (β-C/M) had low β-C degradation after 15 days. The antioxidant properties of the β-C/M were investigated by the 2, 2-diphenyl-1-picrylhydrazyl (DPPH) method and ferric reducing antioxidant power (FRAP) method, respectively. Significantly improved antioxidant activity was observed for β-C/M in compare with free β-C. The aqueous dispersion of β-C/M has potential to be applied in the field of functional food and cosmetics.

1. Introduction

β-C, a well-established natural antioxidant agent, is widely applied in the field of food (Prieto, Rodriguez-Amado, Vazquez, & Murado, 2012; Schreiber, Bozell, Hayes, & Zivanovic, 2013) and cosmetics (Anunciato & da Rocha Filho, 2012). However, β-C is insoluble in water and has very low bioavailability in the crystalline form (Donhowe, Flores, Kerr, Wicker, & Kong, 2014; Donhowe & Kong, 2014). Furthermore, β-C is very sensitive to heat, light and oxygen due to its rich conjugated double bond structure. These drawbacks limit β-C's application as functional ingredient. Fortunately, progresses have been made in improving the solubility and stability of β-C by various strategies. For example, β-C in nanodispersions were prepared and its size distribution was almost unchanged during storage at 4 °C (Tan & Nakajima, 2005). In addition, β-C oil-in-water nanoemulsions were successfully prepared, which had good physical stabilities but, chemically, significant degradation of β-C occurred during storage (Yuan, Gao, Zhao, & Mao, 2008). In a recent example, β-C loaded lipid carriers were prepared with minimum particle size (8–15 nm), low β-C degradation and increased β-C bioavailability (Hejri, Khosravi, Gharanjig, & Hejazi, 2013).

Chitosan (CS), the partly acetylated cationic (1-4)-2-amino-2-deoxy-β-D-glucan, is produced industrially from marine chitin. Its most attractive features are biocompatibility, atoxicity and biodegradability (Muzzarelli, 2009, 2010; Muzzarelli et al., 2012). Recently the application of CS micelles in drug delivery arose great attention (Yang et al., 2014). Many amphiphilic CS derivatives, such as linolenic acid-modified chitosan (Liu, Desai, Chen, & Park, 2005), *N*-alkyl-*N*-trimethyl chitosan (Zhang, Ding, Yu, & Ping, 2007), quaternary ammonium palmitoyl chitosan (Qu et al. (2006) have been applied in carrying hydrophobic drug. Since β-C is also hydrophobic and chemical sensitive with low bioavailability, this work is considering using the self-assembled CS micelles as a substituting nanocarrier for the solubilization and stabilization of β-C. In addition, CS and its derivatives have been reported to possess antioxidant activity (Jarmila & Vavrikova, 2011), thus it is possible to obtain an excellent antioxidant material with the combined effect of β-C and CS micelles.

Amphiphilic CS can be prepared by grafting hydrophobic side chains to CS main chain. Since β-C is mostly applied in food,

Abbreviations: β-C, β-carotene; CS-g-PLA, chitosan-g-poly(lactide); ROP, ring-opening polymerization; β-C/M, β-carotene loaded micelles; DPPH, 2,2-diphenyl-1-picrylhydrazyl; FRAP, ferric reducing antioxidant power; EE, entrapment efficiency; LC, loading content.

* Corresponding authors at: State Key Laboratory of Pulp and Paper Engineering, South China University of Technology, Guangzhou, 510640, China.
Tel.: +86 20 87111861; fax: +86 20 87111861.
E-mail addresses: fewangxh@scut.edu.cn, alicewang1225@163.com (X. Wang).

http://dx.doi.org/10.1016/j.carbpol.2014.09.056
0144-8617/

pharmaceuticals and cosmetics industries, the modifying groups should also be biocompatible and degradable. PLA is a Food and Drug Administration (FDA) approved aliphatic polymer derived from agricultural sources (Jeevitha & Amarnath, 2013). It possesses biodegradability, biocompatibility, good mechanical properties and low hydrophilicity (Yan et al., 2009), and has been widely applied as the hydrophobic component of amphiphilic copolymers. In the current work, amphiphilic CS was prepared by homogeneous grafting PLA side chains on the CS backbone. The self-assembled nanomicelles of CS-graft-PLA copolymer were investigated as the capsules of β-C. The stability and antioxidant activity of β-C encapsulated by CS-g-PLA micelles were studied using the widely accepted DPPH (Gil, Tomas-Barberan, Hess-Pierce, & Kader, 2002) method and FRAP method (Guo et al., 2003). The CS based micelles may extend the application of β-C in functional food and cosmetics industries.

2. Materials and methods

2.1. Materials

CS (deacetylation degrees > 90%) was purchased from Aoxing Biotechnology Co., Ltd. (Zhejiang, China), with average molecular weight of 5 kDa and polydispersity index of 1.6. L-lactide was supplied by Jinan Daigang Biomaterial Co., Ltd. (Jinan, China). 1-Allyl-3-methylimidazolium chloride (AmimCl) with purity of 99% was obtained from Chengjie Chemical Co., Ltd. (Shanghai, China). β-C with purity of 97% was purchased from Tokyo Kasei Kogyo Co., Ltd. (Tokyo, Japan). Stannous octanoate ($Sn(Oct)_2$) (purity > 95%), DPPH and 2,4,6-Tris (2-pyridy)-*s*-triazine (TPTZ) were purchased from Aladdin-reagent Inc. (Shanghai, China). All the other solvents were of analytical reagent grade and used directly without further purification.

2.2. Chemical modification of CS

The PLA grafted CS copolymer was synthesized via homogeneous ROP in ionic liquid. The detailed preparation process for CS-g-PLA copolymer was as follows: 1.0 g CS was added to 10.0 g AmimCl in a 25 mL dried three-neck flask. The mixture was vigorously stirred at 80 °C for 4 h with the protection of nitrogen to make a homogeneous solution. Then the monomer of L-lactide and 0.2% $Sn(Oct)_2$ were slowly added into the solution, and the graft polymerization reaction was carried out at 130 °C under nitrogen for a further 24 h. After cooling to room temperature, the resultant solution copolymer was precipitated with ethanol, and then extracted with acetone at 80 °C for 24 h. The final product was dried in vacuum oven at 60 °C for 48 h.

2.3. Characterization of CS-g-PLA copolymer

The chemical structure of the obtained product was characterized by FT-IR and ^{1}H NMR. The FT-IR spectra of pure CS and its derivatives were recorded on a Bruker spectrometer (TENSOR27, Switzerland) in KBr discs at wavelengths in the range of 500–4000 cm^{-1} with 32 times. ^{1}H NMR spectra measurements were executed on a Bruker DMX500 NMR Spectrometer (Germany) operating at 250 MHz, using DMSO-d_6 as solvent and tetramethylsilane (TMS) as an internal standard. Then according to the peak assignments of ^{1}H NMR spectra, the structural factors of CS-g-PLA copolymer were estimated with Eqs. (1)–(4) (Duan et al., 2010; Guo, Wang, Shu, Shen, & Sun, 2012b):

$$\mathrm{MS} = \frac{\text{lactyl units}}{\text{glucosamine}} = \frac{I_{(a+a')}}{I_{(3,4,5,6)}/5} \quad (1)$$

$$\mathrm{DS} = \frac{\text{terminal lactyl untis}}{\text{glucosamine}} = \frac{I_{a'}}{I_{(3,4,5,6)}/5} \quad (2)$$

$$\mathrm{DP_{PLA}} = \frac{\mathrm{MS}}{\mathrm{DS}} = \frac{I_a}{I_{a'}} + 1 \quad (3)$$

$$W_{\mathrm{PLA}} = \frac{72\mathrm{MS}}{161 + 72\mathrm{MS}} \times 100\% \quad (4)$$

where MS, DS, DP_{PLA}, W_{PLA} are the molar substitution of PLA, the degree of substitution of PLA, the degree of polymerization of PLA, and the weight content of PLA side chains, respectively. The 72 and 161 g/mol in Eq. (4) are the molecular weights of L-lactide monomer and CS repeating unit, respectively.

The crystal structure of CS and the copolymer was characterized by XRD Spectroscopy on a D8 ADVANCE X-ray diffractometer (Germany), in which the high-intensity monochromatic nickel-filtered Cu *K*α radiation was generated at 40 kV and 40 mA. Samples were scanned at a scanning speed of 1°/min, range from 2θ = 5–60° with step size of 0.02° at room temperature.

The thermal stability was determined by thermogravimetric analysis (TGA) (TGA Q500, TA, USA). Each sample (5 mg) for testing was heated in an aluminum crucible to 600 °C at a heating rate of 10 °C/min while the apparatus was continually flushed with a nitrogen flow of 25 mL/min.

2.4. Critical micelle concentration (CMC) measurement

The CMC value was determined by using pyrene as a hydrophobic probe with fluorescence spectroscopy (Jobin-Yvon Fluorolog Tau-3, America). A serial dilution of polymeric micelles was prepared in aqueous solutions at various concentrations ranging from 10^{-5} mg/mL to 1 mg/mL. A known amount of 6×10^{-5} M pyrene/THF solution was added to each micelle solution (Guo et al., 2012b), and the THF was allowed to evaporate to make the final concentration of pyrene in micelle solution to be 6×10^{-7} M. Then the sample solutions were sonicated for 30 min at room temperature to equilibrate pyrene. The emission spectra of the solutions were recorded from 360 to 550 nm with an excitation wavelength of 339 nm. Peak height intensity ratio (I_1/I_3) of the first peak (I_1 at 375 nm) to the third peak (I_3 at 386 nm) was plotted against the logarithm of polymer concentration. The CMC value was taken from the intersection of the tangent to the curve at the inflection with the horizontal tangent through the points at low concentrations.

2.5. Preparation of blank micelles and β-C/M

The form of blank CS-g-PLA micelles in aqueous solutions was triggered by the sonication of copolymer's water solution by using a probe type sonicator (VCX750, Sonics and materials Inc., USA) in an ice bath. In detail, 10 mg CS-g-PLA copolymer was dissolved in 10 mL ultrapure water. Subsequently, the copolymer's aqueous solution was ultrasonicated at amplitude of 40 (750 W, 20 kHz) for 30 min before analysis. The pulse function was pulse on 2 s and pulse off 2 s.

The β-C/M was prepared though microphase separation method. Briefly, 10 mg CS-g-PLA copolymer was dissolved in 10 mL ultrapure water. Subsequently, 2 mL THF dissolving β-C was added dropwise into the polymer solution to give the final feed concentration of β-C ranging from 0.05 to 2.0 mg/mL while being sonicated for 30 min by a probe-based sonicator. Then, the organic solvent was removed from the mixture solution at 37 °C by rotary evaporation. The solution was consequently adjusted to CS-g-PLA concentration of 1 mg/mL and filtered through a 0.45 μm membrane filter to remove free β-C. The resultant solution was stored at 4 °C for subsequent analysis.

The absorbance of the resultant solution was measured by a UV–vis spectrophotometer at 457 nm. The concentration of β-C was calculated according to a standard curve. The entrapment efficiency (EE) and loading content (LC) of β-C encapsulated in CS-g-PLA micelles were then determined according to Eqs. (5) and (6), respectively.

$$\text{EE}\ (\%) = \frac{\text{weight of loaded}\ \beta\text{-C}}{\text{weight in control}} \times 100\% \quad (5)$$

$$\text{LC}\ (\%) = \frac{\text{weight of loaded}\ \beta\text{-C}}{\text{weight of polymer}} \times 100\% \left(\frac{g}{g}\right) \quad (6)$$

In addition, the stereoisomers of β-carotene, i.e. cis and trans isomers, have different absorption values and corresponding wavelengths. Although, the changes of the stereochemical conformation occur under illumination and thermal treatment, these transformations at room temperature were disregarded in our studies (Chen, Chen, & Chien, 1994).

2.6. Physiochemical properties of β-C/M

The size and zeta potential of blank polymer micelles and β-C/M were investigated by dynamic light scattering (DLS) on a Zetasizer 3000 HS instrument (England) at 90° scattering angle at 25 °C. The morphology of the CS-g-PLA micelles was observed by TEM (JEM-2100, Japan). A drop of sample was placed onto the copper grids coated with carbon film. The sample was negatively stained with phosphotungstic acid and dried at room temperature before observation.

2.7. Stability of β-C/M

The prepared β-C/M was poured into a brown vial and stored in a temperature-controlled incubator at 4 °C and 25 °C for 3, 6, 9, 12, and 15 days, respectively. After the desired temperature and storage time were reached, the stabilities of samples were investigated. The particle size and polydispersity index (PDI) were conducted by DLS, while the concentration of β-C entrapped in micelles during storage. The concentration of β-C was measured at 457 nm using a UV–vis spectrophotometer. Eq. (7) was used to calculate the degradation rate.

$$\text{Retention rate}\,(\%) = \frac{C_0 - C}{C_0} \times 100\% \quad (7)$$

where C_0 and C are initial concentration and concentration after storage of β-C located in micelles, respectively. Then a first-order degradation equation was expressed as $\ln(C/C_0) = -kt$, where k was the apparent reaction rate constant (per day), and t was the days of storage (Sharma & Le Maguer, 1996).

2.8. Evaluation of antioxidant capacity

Briefly, a determined concentration of sample solution was mixed with 2 mL 4 mg/mL DPPH ethanol solution and left at room temperature in the dark for specific time (Sharma & Bhat, 2009). Then the absorbance of the resulting solution was measured at 517 nm with UV–vis assay. The DPPH radical scavenging effect was calculated according the following equation:

$$\text{DPPH radical scavenging activity}\,(\%) = \frac{A_0 - A_1}{A_0} \times 100\% \quad (8)$$

where A_0 is the absorbance of the control, A_1 is the absorbance of the sample.

FRAP value was determined through a previously reported method (Benzie & Strain, 1996) with slight modification. In brief, the FRAP reagent was prepared freshly by mixing 10 mM TPTZ, 20 mM ferric chloride and 300 mM acetate buffer (PH 3.6) in a ratio of 1:1:10 (v/v/v). Then a determined amount of free β-C, β-C/M and blank CS-g-PLA micelles with concentration of 1 mg/mL was mixed with 4.5 mL FRAP reagent and incubated at 37 °C for specific times, respectively. The absorbance of the resulting solution at 593 nm was monitored by UV–vis spectrophotometer. The FRAP values were evaluated based on a calibration curve.

2.9. Statistical analysis

Each analysis was carried out in triplicate and all data were expressed as mean value ± standard deviation (SD). SPSS 19.0 was used to analyze the data. ANOVA was performed to determine the least significance at $p < 0.05$.

3. Result and discussion

3.1. Synthesis of CS-g-PLA copolymer

Scheme 1a illustrates the synthesis route of CS-g-PLA copolymer. Ionic liquid, as a much stronger hydrogen bond acceptor, can interact with the amino or hydroxyl groups of CS resulting in efficient dissolving of CS at comparably mild conditions and also can effectively dissolve most modifying monomers. In the reaction, CS and L-lactide were dissolved in AmimCl to form homogeneous system for ROP. Furthermore, $Sn(Oct)_2$ was applied as an assistant catalyst to co-initiate the ROP of L-lactide with the hydroxyl or amino group of CS.

3.2. Characterization of CS-g-PLA copolymer

Fig. 1A shows the normalized FT-IR spectra of CS and CS-g-PLA copolymer. According to Fig. 1A, the main adsorption bands at 3448 cm^{-1} (combined peaks of the NH_2 and OH group), 2930 cm^{-1} and 2880 cm^{-1} (C—H stretch of CH_2 symmetry), 1655 cm^{-1} (—C=O stretch of amide bonds —$CONH_2$) can be observed in the spectra of CS. Compared with the spectra of unmodified CS, new bands attributing to the carbonyl stretch at 1743 cm^{-1}, the symmetric C—O—C at 1207 cm^{-1} and the CH_3 stretch vibrations of the PLA grafts at 2934 cm^{-1} present in the spectra of CS-g-PLA copolymer. This indicated that the polymer of PLA was successfully grafted onto CS backbone via ROP (Guo, Wang, Shu, Shen, & Sun, 2012a; Li et al., 2012).

The ^1H NMR spectra of CS-g-PLA copolymer is shown in Fig. 1B. The resonance peaks at 4.79, 3.6–3.3, and 3.10 ppm are attributed to the H_1, $H_{3,4,5,6}$, and H_2 in the CS units, respectively. The signals derived from the C_3—OH and C_6—OH protons of residual hydroxyl in CS appear at 5.43 and 4.34 ppm, respectively. The new peaks at 1.29 and 1.05 ppm correspond to the internal and terminal methyl protons (H_b and $H_{b'}$) of PLA side chain, respectively, whereas the chemical shifts at 5.00 and 4.19 ppm are ascribed to the internal and terminal methylene protons (H_a and $H_{a'}$) of PLA side chain, respectively. These results demonstrated that the CS-g-PLA copolymer was successfully synthesized by ROP, which was consistent with the result of FT-IR spectra. Moreover, the calculated values of MS, DS, DP_{PLA} and W_{PLA} for synthesized CS-g-PLA copolymers are 2.82, 1.93, 1.47 and 55.77%, respectively.

Fig. 1C shows the XRD patterns of CS and CS-g-PLA copolymer. The crystalline character of CS can be established with the main diffraction signals appearing at around 2θ of 10.45°, 19.97°, and 22.05°, respectively. However, the diffraction peak at 10.45 °for CS is absent, while another broad peak at 2θ of 20.16° showing an amorphous character appear in the XRD pattern of CS-g-PLA copolymer. This indicated that the chemical modification had destroyed the hydrogen bondings between CS molecules and decreased the original crystallinity of CS (Thammawong et al., 2012).

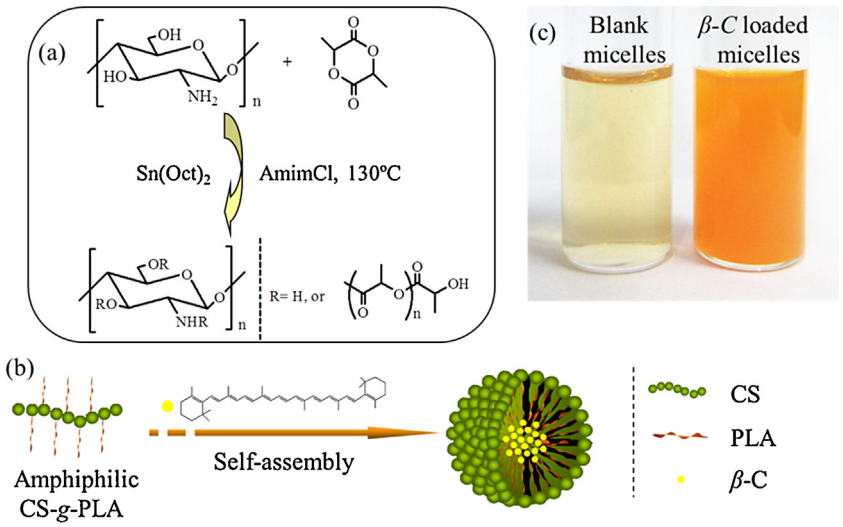

Scheme 1. Synthesis of CS-g-PLA in ionic liquid AmimCl (a). The formation of β-C/M (b). Appearance of blank micelles and β-C/M (c).

The TGA in nitrogen atmosphere were performed with CS and graft copolymer, as shown in Fig. 1D. It can be seen that the unmodified CS has followed one main decomposition step and near 41% of weight has decomposed at 360 °C, which is responsible for the thermal decomposition of glucosamine residue. In the case of CS-g-PLA copolymer, one decomposition step with 52% weight loss at 345 °C is occurred. The DTG curves show that the maximum decomposition rate of CS occurs in the peak of 285.6 °C, while the maximum decomposition rate of the graft copolymer occurred via a sharp peak at 260.3 °C. These results suggested that the graft modification resulted in a scarified thermal stability of CS-g-PLA copolymer. It is probably due to that the crystalline structure in CS had been partially destroyed by the introduction of PLA chains, the modified CS with looser and disordered crystalline structure were more easily decomposed by thermal treatment (Guo et al., 2012a).

3.3. Self-assembly behavior of CS-g-PLA copolymer

The photoluminescence of pyrene is very sensitive to the polarity changes of surrounding environment. Owing to its hydrophobic nature, pyrene would be preferentially located in the hydrophobic core of the micelle. Then the photophysical properties of pyrene would show significant changes, as shown in Fig. 2A. The intensity ratio of 375 nm and 386 nm I_1/I_3 in pyrene's emission spectrum is

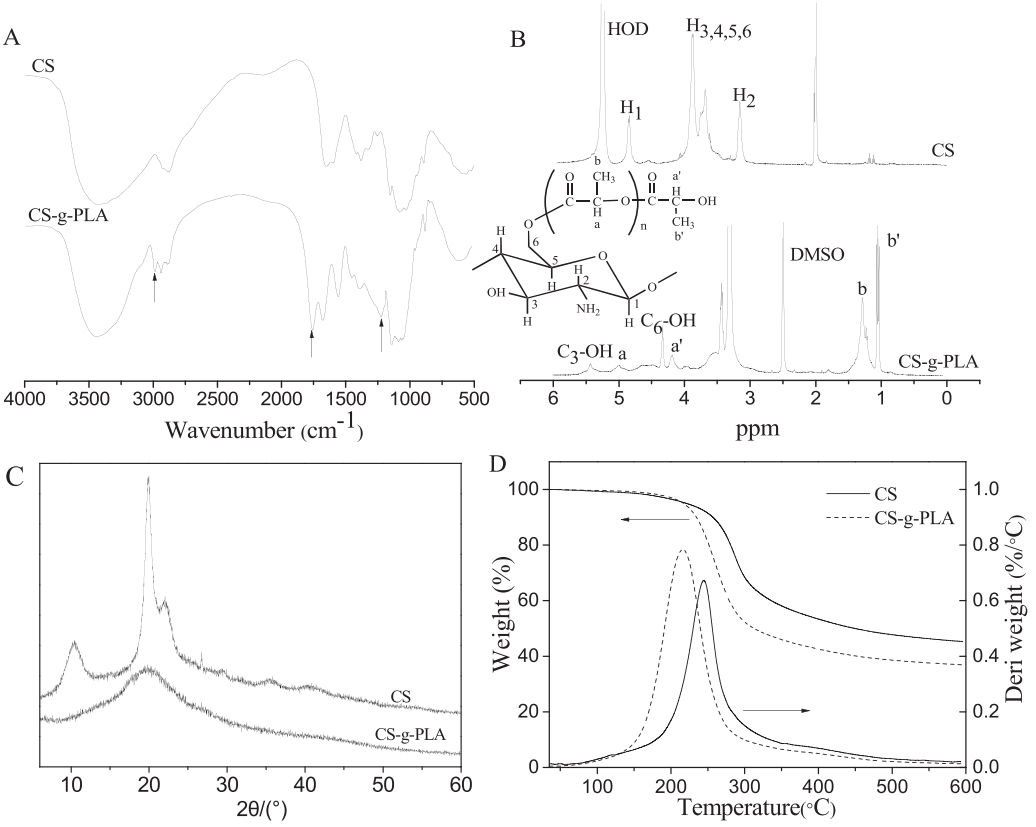

Fig. 1. Characterizations of CS and CS-g-PLA: FT-IR spectra (A), ^{1}H NMR spectra (B), XRD (C) and TGA (D).

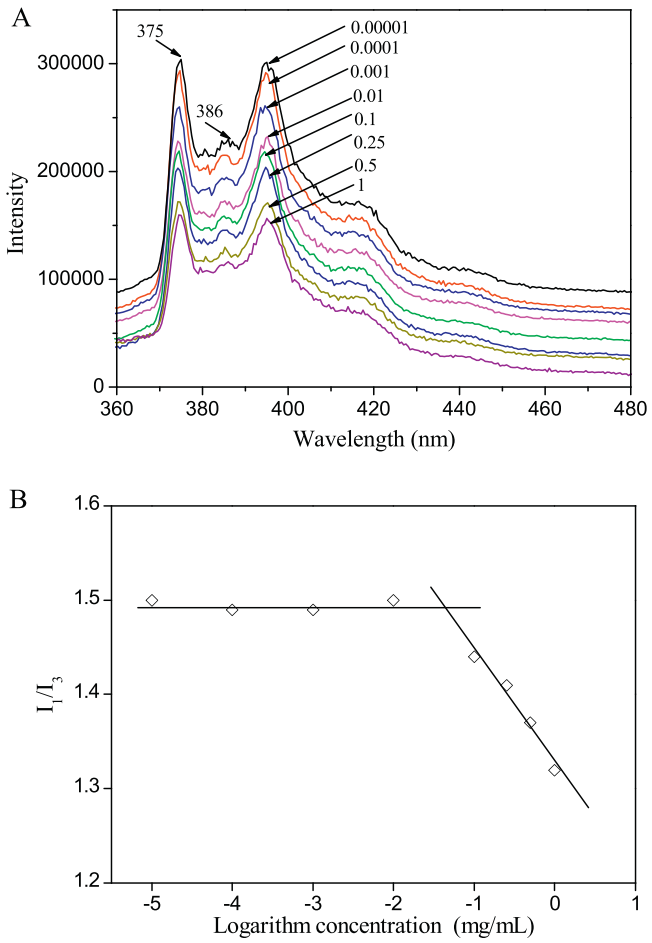

Fig. 2. Pyrene emission spectra of CS-g-PLA solutions with different concentrations (mg/mL) (A). Intensity ratio (I_1/I_3) of the pyrene emission spectra versus of the logarithm concentration of CS copolymer (B).

usually used as the index to measure the polarity of microenvironment. Fig. 2B exhibits the value of I_1/I_3 versus the log concentrations of CS-g-PLA copolymers in water. As shown, the I_1/I_3 kept constant at low concentration before reaching a limit value. The limit concentration is recognized as the CMC of the amphiphilic polymer. The CMC value of the CS-g-PLA was calculated to be 0.035 mg/mL.

An ultrasonication method was taken in this study to prepare the self-assembled micelles of CS-g-PLA copolymer. The particle size and PDI of the resulting self-assembled nanomicelles were evaluated by DLS techniques. Fig. 3A shows the size histogram of CS-g-PLA micelles by number. In addition, the DLS results show that the average particle size is 14.33 ± 0.528 nm and PDI of 0.184 ± 0.046, thus the nanomicelles exhibit narrow size distribution. The morphology of the CS-g-PLA nanomicelles was observed by TEM, as depicted in Fig. 3B. It can be seen that the self-assembled CS-g-PLA micelles are well-distributed with spherical nanosized structure. The observed micelle size of CS-g-PLA micelles is about 14 nm, which is consistent with the result of DLS analysis.

3.4. Encapsulation of β-C in CS-g-PLA nanomicelles

β-C is a highly lipophilic non-polar organic compound made up of multiple isoprenoid unites as shown in Scheme 1b. Upon dispersed in the micelle's water solution, β-C tend to precipitate in the hydrophobic domain within micelle core, and thus be physically encapsulated in the micelles, as shown in Scheme 1c. The EE and LC of β-C/M were indirectly obtained by measurement the samples absorption using a UV–vis spectrophotometer at 457 nm. Fig. 4A shows the effect of β-C initial concentration on the loading capacity of CS-g-PLA nanomicelles. As shown, the EE of CS-g-PLA micelles undergoes an obvious decline from 59.17 to 24.67% with increasing feed concentration of β-C from 0.05 to 2 mg/mL. On the other hand, the value of LC indicating the exact amount of β-C located in CS-g-PLA micelles is significantly enhanced from approximately 3 to 50% with the initial concentration of β-C increased from 0.05 to 2 mg/mL. This indicated that the CS-g-PLA micelles had a high LC for β-C, but over high initial concentration would result in low EE. Taking into consideration both of the EE and LC values, the initial concentration of 1 mg/mL was a proper condition, at which the EE and LC of nanomicelles both reached 36.21 ± 4.64%. Thus, the optimum initial concentration of β-C (1 mg/mL) was chosen for subsequent studies.

3.5. Characterization of β-C loaded CS-g-PLA micelles

The particle size and solution properties of β-C/M with different β-C loading amount were investigated through DLS. Fig. 4B shows the influence of β-C loading amount on particle size and zeta potential. As shown, the size of β-C/M is obviously larger than the blank micelles, indicating that β-C has been successfully entrapped in CS-g-PLA micelles, and the entrapment process is probably accompanied by an expansion of micelle core. It is also noticed that the colloidal particle size of nanomicelles significantly increase from 64.72 to 169.91 nm with concentration of β-C increasing from 29.6 to 493.4 μg/mL. This result demonstrated that as the CS-g-PLA nanomicelles containing more β-C had a larger particle size. It is possible due to the inter- & intra-aggregate forces and their balance determining the aggregate structure is changed with the introduction of β-C (Rodriguez-Hernandez, Checot, Gnanou, & Lecommandoux, 2005). With the introduction of β-C, the PLA blocks forming the core will be more stretched and the interaction between CS main chains forming the corona will be reduced.

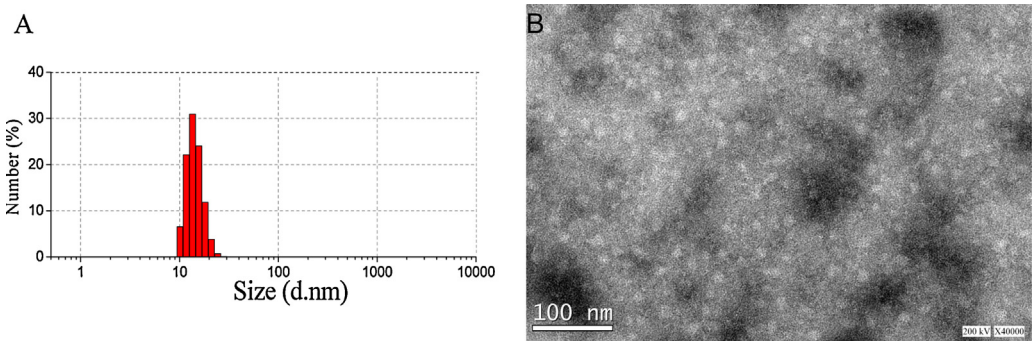

Fig. 3. The size histogram of CS-g-PLA micelles determined by DLS (A) and TEM image (B).

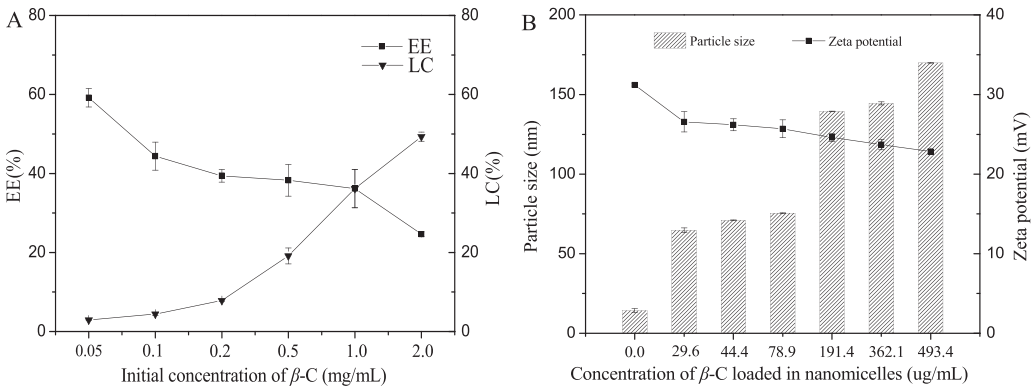

Fig. 4. EE and LC of CS-g-PLA nanomicelles with different initial concentrations of β-C (A). Particle size and zeta potential of β-C loaded CS-g-PLA nanomicelles with different loading amount of β-C (B).

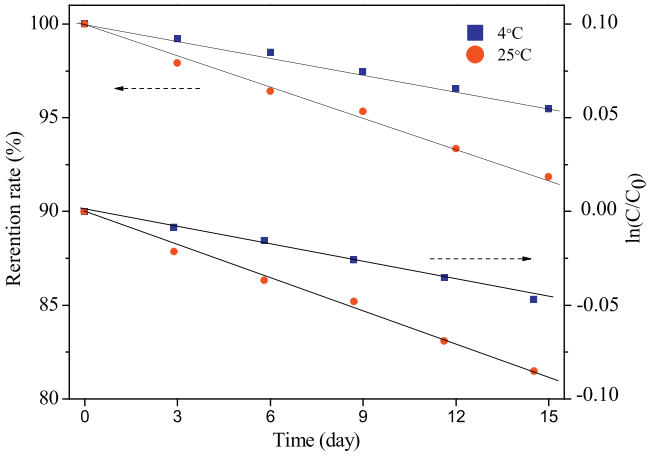

Fig. 5. Degradation curve and degradation kinetics curve of β-C located in CS-g-PLA micelles during storage at 4 °C and 25 °C.

This hypothesis may be proved by the difference in zeta potential between blank micelles and β-C/M. As shown, the zeta potential of CS-g-PLA micelles decreases from 31.2 to 23.8 mV, when the initial concentration is increased from 0.0 to 493.4 μg/mL. This result indicated a decrease of the surface charges on the micelles with increasing β-C content. The decrease of zeta potential could be due to the increase of particle size induced by an increase of β-C concentration has retarded the electrophoretic mobility of the particle (Lee, Kim, & Lee, 2010).

3.6. Stability of β-C/M

In this paper, investigations on their physical stability showed no significant change in particle size distributions of samples over a storage time of 15 days at different storage temperature, as shown in Table 1. The retention rate of β-C located in micelles during storage is shown in Fig. 5. Overall, a decreasing trend was found following the increase of both storage time and temperature. After storage at 4 and 25 °C for 15 days, the β-C/M showed a loss of 4.55% and 8.15%, respectively. In the kinetic study, a first-order reaction curve is shown for the concentration changes of β-C in the micelles at each temperature. It indicates that the amount of β-C followed a decreasing trend with higher storage temperature.

3.7. Antioxidant study

The DPPH radical scavenging activities of β-C/M micelles as a function of β-C concentration and time are presented in Fig. 6. As shown in Fig. 6A, during the determination time, the DPPH radical scavenging activities by free β-C and β-C/M increased with the concentration ranging from 51 to 411 μg/mL, which reflect the concentration-dependent antioxidant activity of free β-C and β-C/M. Moreover, there was a significant difference in DPPH radical scavenging capacity for the enhancement of β-C/M antioxidant capacity compared to free β-C. From Fig. 6B, a similar increasing variation trend of DPPH radical scavenging abilities of β-C/M can be observed. However, β-C/M exhibited higher DPPH radical scavenging rate than the free β-C. It can be seen that the high capacity of β-C/M to scavenge almost 100% free radicals in 10 min, while the scavenging activities of the free β-C was less than 60%. The free β-C reached a scavenge free radicals of 91.9% after 120 min. Moreover, the 1 mg/mL blank micelles show antioxidant activity with scavenging DPPH free radical of 62.15%. These results suggested that the β-C/M improved the antioxidant activity of β-C (Lee et al., 2010).

As shown in Fig. 6C, the enhancement of antioxidant activity is identified for both free β-C and β-C/M with increasing concentrations. CS-g-PLA nanomicelles with β-C encapsulation concentration ranged from 51 to 411 μg/mL exhibited FRAP value ranging from approximately 18 to 104 μmol/mL. However, the measured FRAP value of free β-C increased from only 12 to 66 μmol/mL. Fig. 6D shows the antioxidant activity of free β-C, β-C/M and 1 mg/mL blank micelles as a function of time by FRAP method. A steady increase of FRAP value of both free β-C and β-C/M is

Table 1
The particle size and PDI of β-C/M during storage at 4 °C and 25 °C.

Time (day)	4 °C		25 °C	
	Particle size (nm)	PDI	Particle size (nm)	PDI
0	144.374 ± 1.785	0.195 ± 0.029	144.374 ± 1.984	0.195 ± 0.029
3	145.021 ± 1.954	0.205 ± 0.019	144.563 ± 1.996	0.204 ± 0.056
6	145.210 ± 1.965	0.186 ± 0.039	145.011 ± 2.201	0.215 ± 0.055
9	144.781 ± 2.201	0.199 ± 0.081	144.785 ± 2.246	0.209 ± 0.068
12	144.532 ± 1.798	0.218 ± 0.034	145.352 ± 2.465	0.220 ± 0.085
15	145.321 ± 1.154	0.209 ± 0.045	145.012 ± 2.365	0.232 ± 0.094

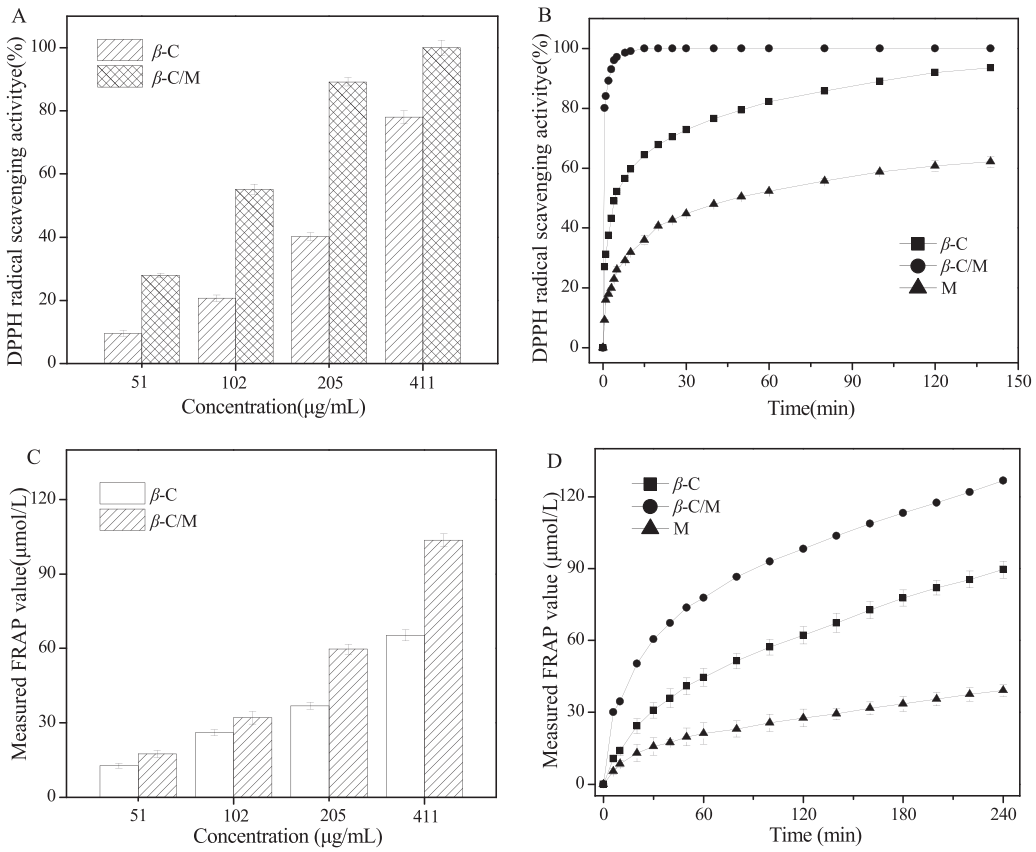

Fig. 6. DPPH radical scavenging activities (A) and measured FRAP value (C) of free β-C and β-C/M with different concentrations. DPPH radical scavenging activities (B) and FRAP value (D) of 411 μg/mL free β-C, β-C/M and 1 mg/mL blank micelles as a function of time.

observed. Compared to the free β-C, β-C/M with the same concentration presented a higher FRAP value at determined time, which meant higher antioxidant ability. And the blank micelles also have a FRAP value of 39 μmol/L and exhibit antioxidant ability. The results of FRAP method were consistent with those of the DPPH assay.

Thus, the results can be conducted that β-C/M not only maintained the intrinsic antioxidant activity of β-C, but also show improved antioxidant activity in aqueous environment. The improved antioxidant activity may be due to multiple factors. On the one hand, the water solubility of β-C was enhanced by nanomicelles encapsulation, which was shown to produce increased availability in aqueous systems (Lee et al., 2010). On the other hand, CS derivatives may express antioxidant activity because the active amino and hydroxyl groups on CS molecular main chain can react with free radical (Schreiber et al., 2013). These results clearly demonstrate that the antioxidant activity of β-C can be effectively improved by CS-g-PLA nanomicelles encapsulation.

4. Conclusions

In summary, amphiphilic CS-g-PLA copolymer was designed and synthesized via ROP, and its fine structure was confirmed with FT-IR and ^{1}H NMR. The CS-g-PLA copolymer with very low CMC was able to self-assemble into micelles in aqueous solution. Moreover, the particle size of β-C/M was almost unchanged while the β-C located in micelles had 4–8% degradation during storage for 15 days. In the antioxidant study, both free β-C and β-C/M exhibited concentration- and time-dependent antioxidant activity by DPPH method and FRAP method. However, the antioxidant activity of β-C was effectively enhanced when it was entrapped within CS-g-PLA nanomicelles. The employment of CS-g-PLA nanomicelles encapsulation provides more potential for improving and extending of the actual applications of β-C.

Acknowledgements

This work was supported by the grants from the National Natural Science Foundation of China (51103046), China Education Ministry, Program for New Century Excellent Talents in University (NCET-13-0215) and the Fundamental Research Funds for the Central Universities, SCUT (2013ZM0053).

Appendix A. Supplementary data

Supplementary data associated with this article can be found, in the online version, at http://dx.doi.org/10.1016/j.carbpol.2014.09.056.

References

Anunciato, T. P., & da Rocha Filho, P. A. (2012). Carotenoids and polyphenols in nutricosmetics, nutraceuticals, and cosmeceuticals. *Journal of Cosmetic Dermatology*, *11*(1), 51–54.

Benzie, I. F., & Strain, J. (1996). The ferric reducing ability of plasma (FRAP) as a measure of antioxidant power: The FRAP assay. *Analytical Biochemistry*, *239*(1), 70–76.

Chen, B. H., Chen, T. M., & Chien, J. T. (1994). Kinetic model for studying the isomerization of a- and b-carotene during heating and illuminatio. *Journal of Agricultural and Food Chemistry*, *42*, 2391–2397.

Donhowe, E. G., Flores, F. P., Kerr, W. L., Wicker, L., & Kong, F. (2014). Characterization and in vitro bioavailability of beta-carotene: Effects of microencapsulation method and food matrix. *LWT-Food Science and Technology*, *57*(1), 42–48.

Donhowe, E. G., & Kong, F. (2014). Beta-carotene: Digestion, microencapsulation, and in vitro bioavailability. *Food and Bioprocess Technology*, *7*(2), 338–354.

Duan, K. R., Chen, H. L., Huang, J., Yu, J. H., Liu, S. Y., Wang, D. X., et al. (2010). One-step synthesis of amino-reserved chitosan-graft-polycaprolactone as a promising substance of biomaterial. *Carbohydrate Polymers*, *80*(2), 498–503.

Gil, M. I., Tomas-Barberan, F. A., Hess-Pierce, B., & Kader, A. A. (2002). Antioxidant capacities, phenolic compounds, carotenoids, and vitamin C contents of nectarine, peach, and plum cultivars from California. *Journal of Agricultural and Food Chemistry*, *50*(17), 4976–4982.

Guo, C. J., Yang, J. J., Wei, J. Y., Li, Y. F., Xu, J., & Jiang, Y. G. (2003). Antioxidant activities of peel, pulp and seed fractions of common fruits as determined by FRAP assay. *Nutrition Research*, *23*(12), 1719–1726.

Guo, Y., Wang, X., Shu, X., Shen, Z., & Sun, R.-C. (2012). Self-assembly and paclitaxel loading capacity of cellulose-graft-poly(lactide) nanomicelles. *Journal of Agricultural and Food Chemistry*, *60*(15), 3900–3908.

Guo, Y., Wang, X., Shu, X., Shen, Z., & Sun, R. C. (2012). Self-assembly and paclitaxel loading capacity of cellulose-graft-poly(lactide) nanomicelles. *Journal of Agricultural and Food Chemistry*, *60*(15), 3900–3908.

Hejri, A., Khosravi, A., Gharanjig, K., & Hejazi, M. (2013). Optimisation of the formulation of beta-carotene loaded nanostructured lipid carriers prepared by solvent diffusion method. *Food Chemistry*, *141*(1), 117–123.

Jarmila, V., & Vavrikova, E. (2011). Chitosan derivatives with antimicrobial, antitumour and antioxidant activities—A review. *Current Pharmaceutical Design*, *17*(32), 3596–3607.

Jeevitha, D., & Amarnath, K. (2013). Chitosan/PLA nanoparticles as a novel carrier for the delivery of anthraquinone: Synthesis, characterization and in vitro cytotoxicity evaluation. *Colloids and Surfaces B—Biointerfaces*, *101*, 126–134.

Lee, J. S., Kim, G. H., & Lee, H. G. (2010). Characteristics and antioxidant activity of *Elsholtzia splendens* extract-loaded nanoparticles. *Journal of Agricultural and Food Chemistry*, *58*(6), 3316–3321.

Li, J., Kong, M., Cheng, X. J., Dang, Q. F., Zhou, X., Wei, Y. N., et al. (2012). Preparation of biocompatible chitosan grafted poly(lactic acid) nanoparticles. *International Journal of Biological Macromolecules*, *51*(3), 221–227.

Liu, C.-G., Desai, K. G. H., Chen, X.-G., & Park, H.-J. (2005). Linolenic acid-modified chitosan for formation of self-assembled nanoparticles. *Journal of Agricultural and Food Chemistry*, *53*(2), 437–441.

Muzzarelli, R. A. A. (2009). Chitins and chitosans for the repair of wounded skin, nerve, cartilage and bone. *Carbohydrate Polymers*, *76*(2), 167–182.

Muzzarelli, R. A. A. (2010). Chitins and chitosans as immunoadjuvants and non-allergenic drug carriers. *Marine Drugs*, *8*(2), 292–312.

Muzzarelli, R. A. A., Boudrant, J., Meyer, D., Manno, N., DeMarchis, M., & Paoletti, M. G. (2012). Current views on fungal chitin/chitosan, human chitinases, food preservation, glucans, pectins and inulin: A tribute to Henri Braconnot, precursor of the carbohydrate polymers science, on the chitin bicentennial. *Carbohydrate Polymers*, *87*(2), 995–1012.

Prieto, M. A., Rodriguez-Amado, I., Vazquez, J. A., & Murado, M. A. (2012). beta-Carotene assay revisited. application to characterize and quantify antioxidant and prooxidant activities in a microplate. *Journal of Agricultural and Food Chemistry*, *60*(36), 8983–8993.

Qu, X., Khutoryanskiy, V. V., Stewart, A., Rahman, S., Papahadjopoulos-Sternberg, B., Dufes, C., et al. (2006). Carbohydrate-based micelle clusters which enhance hydrophobic drug bioavailability by up to 1 order of magnitude. *Biomacromolecules*, *7*(12), 3452–3459.

Rodriguez-Hernandez, J., Checot, F., Gnanou, Y., & Lecommandoux, S. (2005). Toward 'smart' nano-objects by self-assembly of block copolymers in solution. *Progress in Polymer Science*, *30*(7), 691–724.

Schreiber, S. B., Bozell, J. J., Hayes, D. G., & Zivanovic, S. (2013). Introduction of primary antioxidant activity to chitosan for application as a multifunctional food packaging material. *Food Hydrocolloids*, *33*(2), 207–214.

Sharma, O. P., & Bhat, T. K. (2009). DPPH antioxidant assay revisited. *Food Chemistry*, *113*(4), 1202–1205.

Sharma, S. K., & Le Maguer, M. (1996). Kinetics of lycopene degradation in tomato pulp solids under different processing and storage conditions. *Food Research International*, *29*(3), 309–315.

Tan, C. P., & Nakajima, M. (2005). Effect of polyglycerol esters of fatty acids on physicochemical properties and stability of beta-carotene nanodispersions prepared by emulsification/evaporation method. *Journal of the Science of Food and Agriculture*, *85*(1), 121–126.

Thammawong, C., Sreearunothai, P., Petchsuk, A., Tangboriboonrat, P., Pimpha, N., & Opaprakasit, P. (2012). Preparation and characterizations of naproxen-loaded magnetic nanoparticles coated with PLA-g-chitosan copolymer. *Journal of Nanoparticle Research*, *14*(8), 1–12.

Yan, S., Changsheng, L., Yuan, Y., Xinyi, T., Fan, Y., Xiaoqian, S., et al. (2009). Long-circulating polymeric nanoparticles bearing a combinatorial coating of PEG and water-soluble chitosan. *Biomaterials*, *30*(12), 2340–2348.

Yang, Y., Wang, S., Wang, Y., Wang, X., Wang, Q., & Chen, M. (2014). Advances in self-assembled chitosan nanomaterials for drug delivery. *Biotechnology Advances*, *32*(7), 1301–1316.

Yuan, Y., Gao, Y., Zhao, J., & Mao, L. (2008). Characterization and stability evaluation of β-carotene nanoemulsions prepared by high pressure homogenization under various emulsifying conditions. *Food Research International*, *41*(1), 61–68.

Zhang, C., Ding, Y., Yu, L., & Ping, Q. (2007). Polymeric micelle systems of hydroxycamptothecin based on amphiphilic *N*-alkyl-*N*-trimethyl chitosan derivatives. *Colloids and Surfaces B—Biointerfaces*, *55*(2), 192–199.